

Vibrational spectroscopic studies, HOMO–LUMO, conformational, atomic charge and MEP analyses of ethyl 2-(3-benzoylthioureido)-acetate based on DFT calculations

M. EVECEN

Department of Physics, Faculty of Arts and Sciences, Amasya University, Ipekköy, 05000, Amasya, Turkey

The optimized parameters, vibrational frequencies, and corresponding vibrational assignments of ethyl 2-(3-benzoylthioureido)-acetate have been presented and its energetic values have been calculated by using Density Functional Theory. Different basis sets have been used with selected B3LYP theory. The comparisons of the findings show that B3LYP/6-311++G(d,p) level of theory is superior for both the highest occupied molecular orbitals - the lowest-lying unoccupied molecular orbitals gaps and the geometric parameters. With this theory conformational property was obtained with molecular energy profile of the title compound calculations with respect to selected degree of torsional freedom, which was varied from -180° to $+180^\circ$ in steps of 20° . Besides the frequencies, frontier molecular orbitals, bond lengths, bond angles and dihedral angles are calculated using Density Functional Theory and Hartree-Fock methods. In addition, atomic charge and molecular electrostatic potential analysis of the title compound were performed at B3LYP/6-311++G(d,p) level of theory. Results are in well agreement with each other and the experimental data.

(Received November 13, 2015; accepted April 05, 2016)

Keywords: Density Functional Theory, Hartree-Fock, Ethyl, Acetate

1. Introduction

In recent years, thiourea and its derivatives have been to attract attention used in research and technological applications such as in the pharmaceutical industry [1,2], as catalysts in chemical reactions [3-5] and for extraction of toxic metals [6,7]. Thiourea derivatives [8] possess potent anticancer properties and display a wide range of biological activity including antibacterial, anti-fungal, antitubercular, antithyroid, antihelmintic, rodenticidal, insecticidal, herbicidal, and plant growth regulator properties [9–15]. Especially, to synthesize new thiourea derivatives and to investigate their antimicrobial and anti-tumor activities have been studied by S. Saeed et al. [16]. Recently thiourea has also reported as anti-HIV agents [17-19]. The complexes of thiourea derivatives also show broad spectrum of biological activities. High stability and simple synthesis made it possible to use the N-benzoylthiourea group as modifier of silica for complexation gas chromatography [20]. Thiourea with a formula, $SC(NH_2)_2$ is a versatile reagent in organic synthesis [19]. Ethyl 2-(3-benzoylthioureido)-acetate adopts a cis–trans geometry of the thiourea group. The chemical formula of this compound is $C_{12}H_{14}N_2O_3S$, is stabilized by intermolecular hydrogen bonds between the carbonyl O atoms and the H atom of the thioamide group

and by a C—H...S interaction. Molecules are linked by two intermolecular hydrogen bonds (C—H...O and N—H...O) [21]. In previous publication, the X-ray of ethyl 2-(3-benzoylthioureido)-acetate was studied [21]. In spite of its importance, mentioned above, there is no any theoretical calculation on ethyl 2-(3-benzoylthioureido)-acetate has been published yet. The aim of this study is to investigate the spectral and structural properties of the title compound, ethyl 2-(3-benzoylthioureido)-acetate, using the Density Functional Theory (DFT) and Hartree-Fock methods (HF) calculations. In this work, the molecular structure, vibrational spectra and assignments, frontier molecular orbital energies, and conformational properties, atomic charge and molecular electrostatic potential analysis were investigated on ethyl 2-(3-benzoylthioureido)-acetate.

2. Computational methods

The initial molecular geometry was taken from X-ray diffraction experimental results [21]. Geometry optimizations and total energy of all structures have been performed by solving the Kohn-Sham equations [22] in the DFT. Generalized gradient approximations were employed by using Becke's hybrid exchange parameter functional

[23] and Lee-Yang-Parr (LYP) nonlocal correlation functional [24]. After test of structures parameters and energy converge, we have employed 6-311++G(d,p) basis set for the all calculations. All calculation in this study was performed by using Gaussian 09 package [25]. Visualization of the structure and analyses of the outputs have been achieved with ChemCraft software [26]. Vibrational band assignments were made using the Gauss-View molecular visualisation program [27]. We have calculated structures quantities from the computed results. The highest occupied molecular orbital (HOMO) - the lowest-lying unoccupied molecular orbital (LUMO) energy gaps of the ternary clusters are calculated from;

$$gap_{H-L}(eV) = |E(LUMO) - E(HOMO)|$$

which gives indication to determine chemically stable structures. The harmonic frequency calculations have performed at both HF and DFT levels with 6-311++G(d,p) basis sets by using the optimized structural parameters. The obtained vibrational frequencies have scaled by 0.89 for HF and 0.96 for B3LYP.

3. Results and discussions

3.1. Molecular structure

The atomic numbering scheme for the title molecule is shown in Fig. 1. The crystal structure of the title compound is monoclinic and the crystal structure parameters are given $a = 11.908(4) \text{ \AA}$, $b = 7.795(3) \text{ \AA}$, $c = 14.024(5) \text{ \AA}$, $\beta = 95.600(5)^\circ$ and $V = 1295.5(8) \text{ \AA}^3$ as experimental results [21]. The molecule maintains the *cis-trans* geometry of the thiourea moiety. The phenyl ring (C1–C6) and (S1/N1/N2/O1/C6/C7/C8/C9) fragment are each planar with maximum deviation of 0.097 \AA (exp. 0.031 \AA) for C6 atom from the least square plane of the later. The dihedral angle between the two planes is 21.92° (exp. 26.53°). The bond lengths and angles are in normal ranges [28]. As seen in Fig. 1, there are three intramolecular hydrogen bonds, N2—H7...O1 (1.935 \AA), N2—H7...O2 (2.311 \AA) and C9—H9...S1 (3.027 \AA). We can see also one pseudo-six-membered ring (N2/H7/O1/C7/N1/C8) and two pseudo-five-membered ring (N2/H7/O2/C10/C9) and (C9/H9/S1/C8/N2) in Fig. 1.

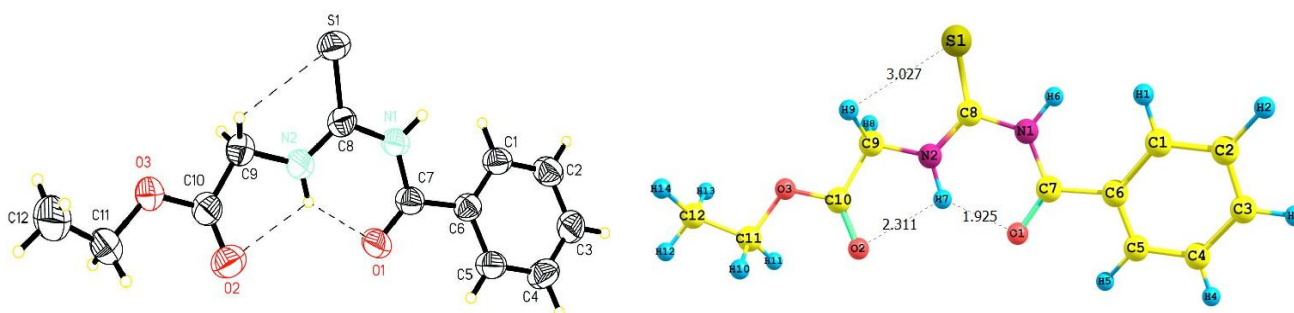


Fig 1. The experimental [21] and the theoretical geometric structures of ethyl 2-(3-benzoylthioureido)-acetate compound (with B3LYP/6-311++G(d,p) level).

Table 1. Energetics of ethyl 2-(3-benzoylthioureido)-acetate for different basis set: Point group (pg), total energy (E_{tot}), total energy+zero point energy ($E_{tot+zpe}$), zero point energy (zpe), minimum frequency (f_{min}), maximum frequency (f_{max}), HOMO energy, LUMO energy and difference between LUMO and HOMO energy (Gap_{H-L}).

	pg	$E_{tot}(eV)$	$E_{tot+zpe}(eV)$	zpe	f_{min}	f_{max}	HOMO	LUMO	Gap (eV)
STO-3G	Cs	-32229.909	-32222.711	7.198	16.380	3733.700	-2.365	0.697	3.062
LANL2MB	Cs	-21790.510	-21783.330	7.181	7.540	3770.530	-3.995	-0.285	3.710
LANL2DZ	Cs	-22066.285	-22059.390	6.895	19.510	3636.180	-5.948	-2.155	3.793
SDD	Cs	-32626.252	-32619.357	6.895	19.330	3635.460	-5.929	-2.125	3.803
3-21G	Cs	-32457.183	-32450.266	6.918	12.720	3573.790	-5.661	-1.793	3.868
6-31G	Cs	-32623.207	-32616.267	6.940	18.450	3635.950	-5.840	-1.938	3.901
6-311G	Cs	-32629.295	-32621.929	6.885	17.340	3621.700	-6.115	-2.153	3.962
cc-pVDZ	Cs	-32631.980	-32625.143	6.837	19.690	3610.710	-5.798	-1.836	3.963
DGDZVP2	Cs	-32635.418	-32628.551	6.868	20.620	3657.020	-6.076	-2.092	3.984
DGDZVP	Cs	-32631.879	-32625.009	6.870	19.760	3616.740	-6.073	-2.046	4.026
6-311++G(d,p)	Cs	-32637.039	-32630.199	6.840	18.848	3622.414	-6.138	-2.087	4.051

The structural parameters are tabulated for different basis set (Table 1). As known, increasing the HOMO-LUMO gaps ($\text{gap}_{\text{H-L}}$) indicate molecules stability. In here, according to $\text{gap}_{\text{H-L}}$, 6-311++G(d,p) basis set is most stable from others (Table 1). So, the most stable optimized

geometry of title molecule, 6-311++G(d,p), is shown in Fig.1. Single point geometries have been determined without any negative frequencies. All of the structures obey C_s symmetry (Table 1).

Table 2. Correlation factors between experimental and calculated values of ethyl 2-(3-benzoylthioureido)-acetate for different basis set.

Basis Sets	Bond				Angle				Torsion Angle			
	b[0]	b[1]	R ²	R	b[0]	b[1]	R ²	R	b[0]	b[1]	R ²	R
LANL2MB	-0.362	1.199	0.956	0.978	17.358	0.852	0.835	0.914	-4.806	0.943	0.993	0.997
LANLZDZ	-0.378	1.230	0.977	0.988	4.043	0.965	0.950	0.975	-3.751	0.960	0.992	0.996
STO-3G	-0.463	1.282	0.979	0.989	18.535	0.843	0.834	0.913	-8.261	1.010	0.982	0.991
3-21G	-0.418	1.269	0.980	0.990	5.597	0.952	0.939	0.969	-4.773	0.943	0.993	0.996
cc-pVDZ	-0.489	1.326	0.982	0.991	5.721	0.951	0.948	0.974	-4.791	0.957	0.988	0.994
6-31G	-0.423	1.272	0.983	0.992	4.325	0.963	0.947	0.973	-4.722	0.958	0.987	0.994
6-311G	-0.413	1.267	0.984	0.992	3.915	0.967	0.940	0.970	-12.100	0.770	0.589	0.767
DGDZVP	-0.460	-0.460	0.985	0.993	5.084	0.957	0.954	0.977	-4.740	0.959	0.986	0.993
SDD	-0.424	1.268	0.987	0.993	4.268	0.963	0.950	0.975	-3.741	0.960	0.992	0.996
DGDZVP2	-0.456	1.302	0.986	0.993	4.755	0.959	0.954	0.977	-4.741	0.957	0.988	0.994
6-311++G(d,p)	-0.457	1.307	0.983	0.992	5.039	0.957	0.956	0.978	-4.746	0.960	0.986	0.993

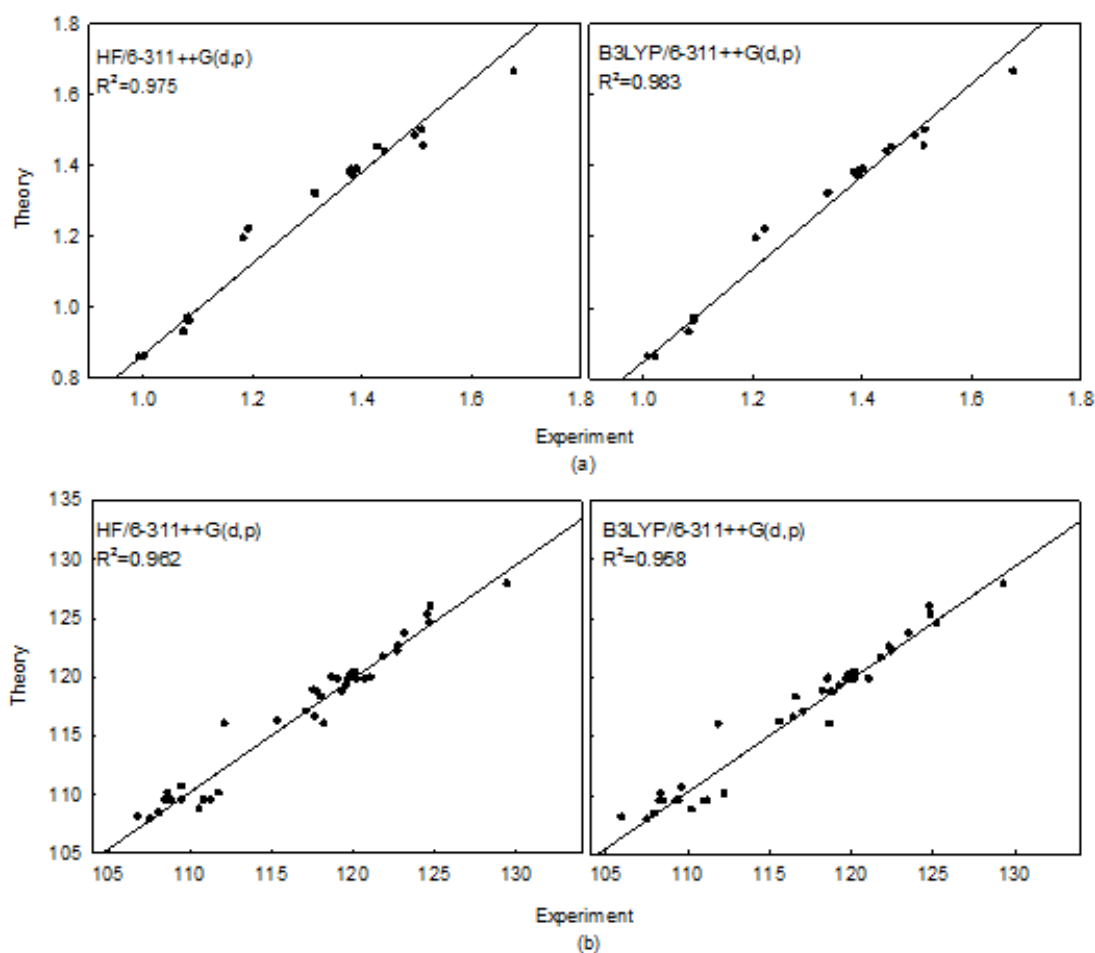


Fig 2. Correlation graphics between experimental and calculated bond lengths (a) and angle (b) for HF/6-311++G(d,p) and B3LYP/6-311++G(d,p) basis sets.

We have also tabulated correlation factors between experimental and calculated values of ethyl 2-(3-benzoylthioureido)-acetate for different basis set in Table 2. Correlation factors between experimental and calculated values for $C_{12}H_{14}N_2O_3S$ is given by $y = b[1]x + b[0]$ formula. In addition to we figured out correlation graphics between experimental and calculated bond lengths and

angle for HF/6-311++G(d,p) and B3LYP/6-311++G(d,p) basis sets in Fig. 2. Our results showed that the differences between experimental and calculated bond lengths of B3LYP are less than HF while there are no significant differences in angles. Furthermore we obtained that B3LYP is more energetic than HF (160.761 eV).

Table 3. Energetics of ethyl 2-(3-benzoylthioureido)-acetate molecule's neutral state(N), anionic state(A) and cationic state(C) for HF and DFT(B3LYP) methods with 6-311++G(d,p).

		pg	$E_{tot}(eV)$	$E_{tot+zpe}(eV)$	zpe	f_{min}	f_{max}	HOMO	LUMO	Gap ^{H-L} (eV)
HF	N	Cs	-32486.787	-32479.438	7.349	21.473	3883.570	-8.958	0.912	9.871
	A	Cs	-32486.797	-32479.610	7.187	14.331	3902.870	-1.838	2.593	4.431
	C	Cs	-32479.999	-32472.714	7.286	20.697	3846.910	-12.885	-1.878	11.006
B3LYP	N	Cs	-32637.039	-32630.199	6.840	18.848	3622.414	-6.138	-2.087	4.051
	A	Cs	-32637.917	-32631.190	6.727	13.012	3641.415	0.327	1.388	1.060
	C	Cs	-32629.067	-32622.255	6.812	18.380	3592.961	-10.536	-6.007	4.529

Moreover, the structural parameters of molecule's neutral state(N), anionic state(A) and cationic state(C) are tabulated for HF and DFT(B3LYP) methods with 6-311++G(d,p) in Table 3. The optimized parameters (bond

lengths, bond angles and dihedral angles) of the title compound have been obtained at HF and B3LYP methods with the 6-311++G(d,p) basis set. Theoretical and experimental geometric parameters are listed in Table 4-6.

Table 4 Experimental and calculated values for bond length.

BOND	Exp.[21]	HF/6-311++G(d,p)			B3LYP/6-311++G(d,p)		
		N (0)	A (-1)	C (+1)	N (0)	A (-1)	C (+1)
S1—C8	1.666	1.679	1.718	1.751	1.678	1.713	1.744
O1—C7	1.221	1.193	1.251	1.184	1.223	1.270	1.211
O2—C10	1.194	1.184	1.182	1.182	1.206	1.202	1.206
O3—C10	1.322	1.313	1.330	1.295	1.340	1.364	1.315
O3—C11	1.452	1.429	1.417	1.448	1.455	1.441	1.478
N1—C7	1.380	1.378	1.444	1.425	1.385	1.430	1.440
N1—C8	1.388	1.382	1.332	1.343	1.402	1.360	1.357
N2—C8	1.32	1.317	1.333	1.288	1.337	1.356	1.310
N2—C9	1.439	1.442	1.432	1.459	1.445	1.429	1.458
C1—C2	1.379	1.385	1.385	1.390	1.392	1.385	1.389
C1—C6	1.390	1.390	1.437	1.402	1.401	1.432	1.405
C2—C3	1.370	1.385	1.405	1.395	1.394	1.405	1.395
C3—C4	1.385	1.387	1.409	1.395	1.395	1.409	1.083
C4—C5	1.379	1.382	1.380	1.390	1.390	1.381	1.388
C5—C6	1.387	1.390	1.438	1.400	1.400	1.432	1.404
C6—C7	1.485	1.497	1.403	1.478	1.498	1.433	1.474
C9—C10	1.500	1.510	1.507	1.520	1.516	1.521	1.534
C11—C12	1.455	1.512	1.514	1.510	1.514	1.517	1.510

Table 5. Experimental and calculated values for bond angles.

ANGLE	Exp.[21]	HF/6-311++G(d,p)			B3LYP/6-311++G(d,p)		
		N (0)	A (-1)	C (+1)	N (0)	A (-1)	C (+1)
C10—O3—C11	118.29	118.085	117.606	118.517	116.654	116.168	117.327
C7—N1—C8	127.91	129.482	128.898	125.994	129.333	129.428	125.700
C8—N2—C9	122.58	122.796	122.823	125.268	122.366	123.949	123.686
C2—C1—C6	120.11	120.116	121.421	120.233	120.229	121.34	119.981
C3—C2—C1	120.33	119.994	121.220	120.004	120.088	121.416	119.958
C2—C3—C4	120.14	120.086	118.526	120.233	119.938	118.084	120.321
C5—C4—C3	119.86	120.000	121.075	120.096	120.101	121.32	120.072
C4—C5—C6	120.32	120.168	121.668	119.786	120.302	121.536	119.930
C5—C6—C1	119.22	119.622	116.078	120.034	119.332	116.296	119.729
C5—C6—C7	117.04	117.168	118.202	116.802	117.089	118.063	116.713
C1—C6—C7	123.72	123.186	125.720	123.143	123.564	125.64	123.549
O1—C7—N1	122.16	122.754	117.425	119.300	122.486	119.152	119.056
O1—C7—C6	121.65	121.850	126.200	125.133	121.872	124.359	125.485
N1—C7—C6	116.19	115.391	116.356	115.558	115.638	116.479	115.446
N2—C8—N1	116.61	117.702	117.994	123.772	116.472	115.687	122.875
N2—C8—S1	124.54	124.709	122.612	120.336	125.239	124.31	119.982
N1—C8—S1	118.83	117.588	119.390	115.891	118.289	120.002	117.139
N2—C9—C10	110.66	109.532	111.337	107.866	109.652	114.324	107.656
N2—C9—H8	109.5	111.353	112.479	111.056	111.168	111.38	111.240
O2—C10—O3	125.96	124.782	123.143	127.437	124.837	123.008	127.665
O2—C10—C9	125.28	124.601	126.872	121.989	124.885	127.699	121.607
O3—C10—C9	108.75	110.616	109.984	110.574	110.278	109.292	110.729
O3—C11—C12	107.90	107.596	107.673	107.501	107.538	107.643	107.427

Table 6 Experimental and calculated values for dihedral (torsion) angles.

TORSION	Exp.[21]	HF/6-311++G(d,p)			B3LYP/6-311++G(d,p)		
		N (0)	A (-1)	C (+1)	N (0)	A (-1)	C (+1)
C6—C1—C2—C3	-0.600	0.374	-0.378	0.244	0.196	-0.376	0.273
C1—C2—C3—C4	0.600	-0.679	-0.513	-0.734	-0.631	-0.371	-0.708
C2—C3—C4—C5	0.500	-0.007	0.536	0.135	0.137	0.462	0.243
C3—C4—C5—C6	-1.500	0.999	0.333	0.947	0.794	0.194	0.652
C4—C5—C6—C1	1.500	-1.298	-1.168	-1.434	-1.221	-0.902	-1.080
C4—C5—C6—C7	-179.660	-179.607	178.914	-179.803	-179.850	-179.060	-179.999
C2—C1—C6—C5	-0.500	0.611	1.188	0.838	0.726	0.991	0.617
C2—C1—C6—C7	-179.210	178.813	-178.900	179.100	-179.261	-178.968	-179.458
C8—N1—C7—O1	-3.000	4.547	17.460	4.580	3.321	4.331	4.507
C8—N1—C7—C6	177.930	-176.209	-164.016	-176.516	177.366	176.771	176.717
C5—C6—C7—O1	-24.700	23.735	4.600	20.811	19.807	3.798	16.764
C1—C6—C7—O1	154.100	-154.509	-175.309	-157.503	158.758	176.244	162.109
C5—C6—C7—N1	154.410	-155.516	-173.776	-158.020	159.510	175.036	161.921
C1—C6—C7—N1	-26.800	26.241	6.315	23.666	21.924	4.922	19.205
C9—N2—C8—N1	-178.790	179.402	-175.734	178.671	-179.652	-174.206	-178.552
C9—N2—C8—S1	2.700	-0.245	4.982	-0.883	-0.207	5.616	-0.730
C7—N1—C8—N2	1.600	0.384	3.389	0.703	-0.307	5.117	-1.930
C7—N1—C8—S1	-179.770	-179.943	-177.303	-179.725	-179.562	-174.713	-177.371
C8—N2—C9—C10	-158.690	179.802	-171.875	-179.165	-179.078	-115.296	-178.826
C11—O3—C10—O2	-1.200	-0.040	-0.051	-0.032	-0.063	1.545	0.013
C11—O3—C10—C9	178.550	179.895	179.663	179.896	179.888	178.212	179.995
N2—C9—C10—O2	2.400	-0.487	-1.006	-0.503	-0.756	6.726	-0.226
N2—C9—C10—O3	-177.340	179.577	179.294	179.564	-179.293	-173.531	-179.782
C10—O3—C11—C12	153.000	-179.999	179.942	179.967	179.847	179.642	179.807

3.2. Vibrational spectra

Harmonic vibrational frequencies were calculated using the HF and DFT/B3LYP method with the 6-311++G(d,p) basis set. Using the Gauss-View molecular visualisation program, the vibrational band assignments were made. The studied title compound $C_{12}H_{14}N_2O_3S$ includes 32 atoms and therefore undergoes 90 normal modes of vibrations. Among the 90 normal modes of vibrations, 61 modes of vibrations are in plane and remaining 29 modes are out of plane. The theoretical frequencies were given in Table 7.

Table 7. Comparison of the calculated vibrational frequencies (cm^{-1}) calculated with HF and B3LYP methods and 6-311++G(d,p) basis set level for the $C_{12}H_{14}N_2O_3S$ molecule's neutral state.

Assignments ^a	B3LYP	HF
ν (N-H)	3279.36	3114.11
ν (C-H) s	3065.28	2914.75
ν (C-H) as	3055.68	2904.96
ν (C-H ₂) as+ (C-H ₃) as	2994.24	2840.88
ν (C-H ₃) as	2981.76	2823.08
ν (C-H ₂) s	2934.72	2791.93
ν (C-H ₂) s	2918.40	2778.58
ν (C-H ₃) s	2917.44	2768.79
ν (C=O)	1724.16	1635.82
ν (C=O)	1655.04	1593.99
ν (C-C) ring	1575.36	1540.59
ν (N-C)	1513.92	1536.14
γ (N-H)	1477.44	1509.44
γ (C-H) ring	1460.16	1467.61
δ (C-H ₃)	1427.52	1444.47
α (C-H ₂)	1423.68	1442.69
ω (C-H ₂) + ω (C-H ₃)	1372.80	1376.83
ω (C-H ₂) + ω (C-H ₃) + ν (C-N)	1352.64	1356.36
ν (C-N)	1334.40	1270.03
ν (C-C)	1207.68	1223.75
ν (C-O) + ω (C-H ₂)	1179.84	1169.46
α (C-H) ring	1160.64	1154.33
ν (C-N)	1141.44	1120.51
ν (C-N) + ν (C-S)	1117.44	1109.83
ω (C-H ₃)	1089.60	1093.81
α (C-H) ring	1067.52	1061.77
ν (C-O) + ν (C-C)	994.56	983.45
ν (C-O-C)	918.72	977.22
ν (C-N-C)	887.04	891.78
ω (C-H ₃)	840.96	837.49
ν (C-S)	773.76	754.72
ω (N-H) + ω (C-H) ring	728.64	740.48
ω (N-H)	596.16	713.78

ν , stretching; δ , twisting; γ , rocking; ω , wagging; α , scissoring; s, symmetric; as, asymmetric.

For fitting the theoretical wavenumbers to the experimental wavenumbers, an overall scaling factor has been introduced by using a least-square optimization of the computed values to the experimental value. Vibrational frequencies is scaled as by 0.89 for HF and 0.96 for B3LYP with 6-311++G(d,p) set [29, 30].

The IR spectra contain some characteristic bands of the stretching vibrations of the C-H, C-H₃, C-H₂, C=O, C-O, C-C, C-N and C-S groups.

C-H vibrations

C-H has a well known characteristic vibrational frequency. Aromatic compounds commonly exhibit multiple weak bands in the region 3100–3000 cm^{-1} value [31] which is the characteristic region for the ready identification of C-H stretching vibrations in plane. In this region the bands are not appreciably affected by the nature of the substituents. Looking to Table 7 we see that the calculated C-H aromatic stretching intensities has a medium intensity and lie within the range 3065–3056 cm^{-1} by B3LYP and 2915–2905 cm^{-1} by HF for which these intensities are in the expected region. Besides C-H in-plane and out-of-plane bending vibrations were lied in the range 1300–1000 cm^{-1} and 950–800 cm^{-1} value [32–34] respectively. In this case, two bands are assigned to C-H in-plane bending vibrations of title compound, identified at 1460 and 1068 cm^{-1} by B3LYP, 1468 and 1062 cm^{-1} by HF in the region. The an out-of-plane wagging bending mode at 728 cm^{-1} by B3LYP, 740 cm^{-1} by HF is observed.

Methyl group vibrations (C-H₃)

The title molecule posses a C-H₃ group. The C-H methyl group stretching vibrations are highly localized and generally observed in the range 3000–2900 cm^{-1} region [35, 36]. In this study, the asymmetric bands with high peaks are found at 2994 and 2982 cm^{-1} by B3LYP and 2841 and 2823 cm^{-1} by HF in the region while it's found at 2917 cm^{-1} by B3LYP and 2769 cm^{-1} by HF simetric stretching vibrations.

In this investigation, C-H₃ four wagging vibration are also found at 1372, 1352, 1089 and 840 cm^{-1} by B3LYP and 1376, 1356, 1093 and 837 cm^{-1} by HF. This assignment authenticated by the literature [37,38].

Methylene vibrations (C-H₂)

In our present work, three wagging, three stretching and a scissoring methylene vibration are found. Generally, the symmetric C-H₂ stretching vibrations are observed between 3000 and 2900 cm^{-1} region [39]. In accordance with this, C-H₂ symmetric mode are observed sharp at 2934 and 2918 cm^{-1} by B3LYP, 2791 and 2778 cm^{-1} by HF while assymmetric mode is observed at 2994 cm^{-1} by B3LYP, and 2840 cm^{-1} by HF. The C-H₂ three wagging out-of-plane deformation vibrations are at 1372, 1352 and 1179 cm^{-1} by B3LYP, at 1376, 1356 and 1169 cm^{-1} by HF.

C=O, C-O vibrations

These vibrations are important to analyze the various factors in ring aromatic compounds. The C=O vibration appears in the expected range shows that it is not much affected by other vibrations [40]. As in literature, the

characteristic infrared absorption frequency of C=O in acids are normally strong in intensity and in the 1800–1690 cm^{-1} region [41]. The carbonyl group vibrations give a characteristic frequency used to study a wide range of compounds. The intensity of these bands can increase because of conjugation or formation of hydrogen bonds [42]. In the present study, three C=O stretching vibrations are identified at 1724 and 1655 cm^{-1} in B3LYP, at 1635 and 1593 cm^{-1} in HF as a strong band because of its large change in dipole moment. Also, C-O vibrations are observed at and 1179 (1169), 994 (983) and 918 (977) cm^{-1} by B3LYP (HF) method which confirms the presence of methoxy group in the compound.

C-N vibrations

In the present study, the identification of C–N stretching vibration is a difficult task due to mixing of vibration. Arslan et al. [41] identified the C–N stretching vibrations in the region 1351–1268 cm^{-1} . Tecklenburg et al. [43] have located the C-N symmetric stretch in the region 1120–1150 cm^{-1} . The C-N stretchings are also found to be present at 1248 and 1199 cm^{-1} by Pajazk et al. [44]. Similarly, in this study, the C–N stretching vibration is observed at 1514, 1353, 1334, 1141, 1117 and 887 cm^{-1} (1536, 1356, 1270, 1121, 1110 and 892 cm^{-1}) by B3LYP (HF).

CC vibrations (C=C and C-C)

The ring C=C and C-C stretching vibrations are expected in the 1620–1390 cm^{-1} region [45]. In general, the bands with variable intensity are observed at 1625–

1590, 1590–1575, 1540–1470, 1465–1430 and 1380–1280 cm^{-1} from the frequency ranges given by Varsanyi [46]. In the present work, the frequencies are observed at 1575, 1208 and 995 cm^{-1} (1541, 1224 and 984 cm^{-1}) have been assigned to C–C stretching vibrations by B3LYP (HF) method and the values are almost in the expected region.

C=S vibration

C=S group is shown absorption bands in broad 1563–700 cm^{-1} region [47]. In our study, C=S stretching band has been calculated at 1117 and 774 cm^{-1} with B3LYP, and 1110 and 754 cm^{-1} with HF.

N-H vibrations

Zhang et al. [48] reported the NH modes at 3467, 1398 and 604 cm^{-1} for a similar studies. In this study, the N–H stretching vibration are characterized by a strong peak appearing at 3279 (3114) cm^{-1} and 1477 (1509) cm^{-1} for B3LYP (HF) method while wagging bands observed at 728 (740) cm^{-1} and 596 (713) cm^{-1} for B3LYP (HF) method. These results also agree with Colthup et al and E.S. Al-Abdullah et. al studies [49, 50].

3.3. Frontier molecular orbitals

The frontier molecular orbitals constitutes basic building block in the electric and optical properties, as well as in UV–vis spectra and chemical reactions [51]. Fig. 3 shows the distributions and energy levels of the HOMO and LUMO orbitals computed at the HF/6-311++G(d,p) and B3LYP/6-311++G(d,p) level for the title compound.

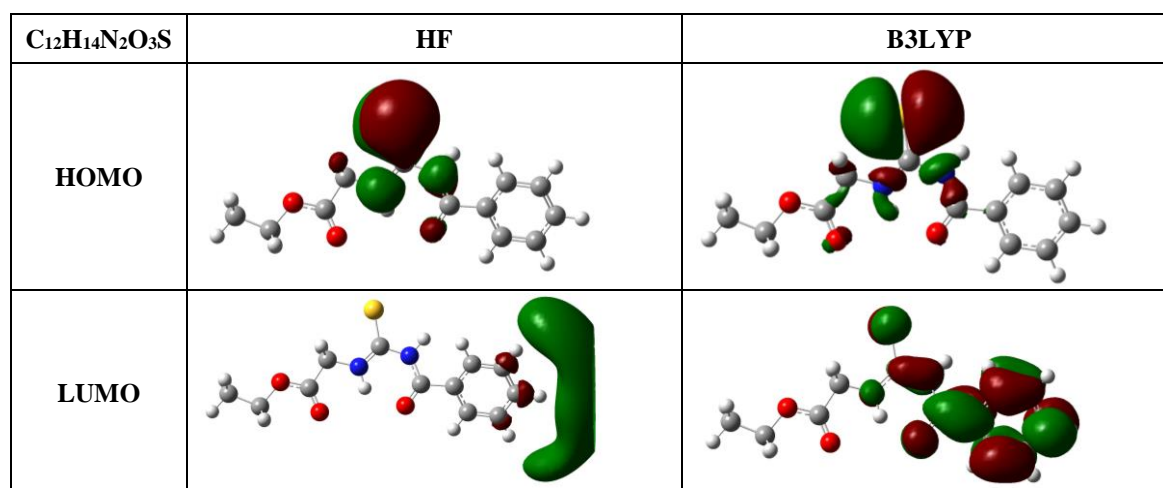


Fig 3. HOMO-LUMO electron density cloud calculated with HF and B3LYP methods and 6-311++G(d,p) basis set level for the $\text{C}_{12}\text{H}_{14}\text{N}_2\text{O}_3\text{S}$ molecule's neutral state.

It is enough to have a glance at Fig. 3 to conclude that the depicted HOMO orbital is lone pairs of the sulfur atom, and the depicted LUMO/HF is a Rydberg orbital. LUMO/B3LYP characteristic behavior is different from LUMO/HF. Although the LUMO cloud covers over phenyl ring with B3LYP, any localization almost has not been observed. The values of the energy separation between the HOMO and LUMO are 9.871 eV and 4.051 eV, respectively. In order to investigate the chemical

stability and reactivity behavior of the title compound, chemical hardness (η) and softness (S) were also investigated with HOMO–LUMO gap. Considering the chemical hardness, small HOMO–LUMO gap ($\Delta E_{\text{H-L}}$) means a soft molecule and large $\Delta E_{\text{H-L}}$ means a hard molecule. One can also relate the stability of the molecule to hardness, which means that the molecule with least $\Delta E_{\text{H-L}}$ means it is more reactive and less stable. The η and S can be calculated using the HOMO and LUMO energy

values for a molecule as follow: $\eta = (E_{\text{LUMO}} - E_{\text{HOMO}})/2$ and $S = 1/2\eta$ [34], where E_{LUMO} and E_{HOMO} are LUMO and HOMO energies, respectively. The calculated values of E_{LUMO} , E_{HOMO} , $\Delta E_{\text{H-L}}$, η and S for the title compound are 0.912 eV, -8.958 eV, 9.871 eV, 4.936 eV and 0.101 eV^{-1} for HF and -2.087 eV, -6.138 eV, 4.051 eV, 2.026 eV and 0.247 eV^{-1} for B3LYP, respectively.

3.4. Conformational analysis

In order to define the preferential position of phenyl ring and ethyl acetate preliminary search of low energy structures was performed using B3LYP/6-311++G(d,p) computations as a function of the selected degrees of torsional freedom $T(\text{N1-C7-C6-C5})$ and $T(\text{C8-N2-C9-C10})$. The respective values of the selected degrees of torsional freedom, $T(\text{N1-C7-C6-C5})$ and $T(\text{C8-N2-C9-C10})$, are 21.92° and 179.08° in DFT optimized geometry. Molecular energy profiles with respect to rotations about the selected torsion angles are given in Fig. 4.a and Fig. 4.b. The obtained results are also tabulated in Table 8 and Table 9. According to the results, the low energy domains for $T(\text{N1-C7-C6-C5})$ are located at 0° , while they are located between at -180° to -60° and between at 75° to 180° for $T(\text{C8-N2-C9-C10})$. Energy difference between the most favorable and unfavorable conformers, which arises from rotational potential barrier calculated with respect to the two selected torsion angles, is calculated as 0.17 eV for $T(\text{N1-C7-C6-C5})$ and as 7.5 eV for $T(\text{C8-N2-C9-C10})$, when both selected degrees of torsional freedom are considered.

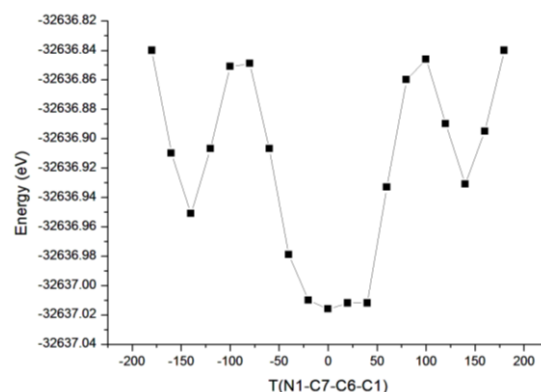


Fig 4. (a) Potential energy profile using B3LYP/6-311++G(d,p) method for the internal rotation around the C7-C6 bond of the title compound.

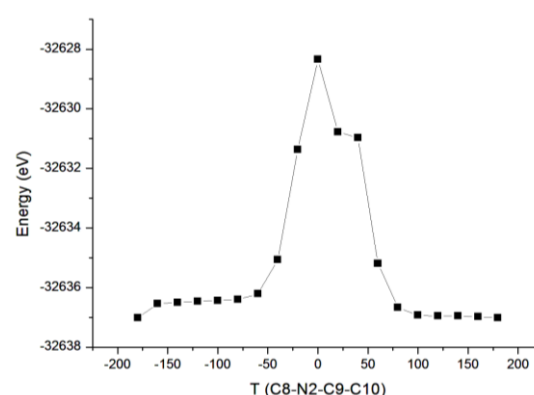


Fig 4. (b) Potential energy profile using B3LYP/6-311++G(d,p) method for the internal rotation around the N2-C9 bond of the title compound.

Table 8 Structural parameters and charges (N1, C7, C6, C5) for $T(\text{N1-C7-C6-C5})$ angles.

Torsion1	E_{tot} (eV)	HOMO	LUMO	$\text{Gap}_{\text{H-L}}$ (eV)	N1	C7	C6	C5
180	-32636.840	-6.138	-2.153	3.985	0.460	0.105	0.612	-0.258
160	-32636.895	-6.141	-2.086	4.055	0.148	-0.316	0.890	-0.492
140	-32636.931	-6.150	-1.925	4.224	0.077	-0.389	0.917	-0.243
120	-32636.890	-6.161	-1.722	4.439	0.043	-0.493	0.839	-0.070
100	-32636.846	-6.169	-1.543	4.626	0.083	-0.736	0.639	-0.060
80	-32636.860	-6.166	-1.559	4.607	0.095	-0.765	0.594	-0.264
60	-32636.933	-6.154	-1.750	4.404	0.035	-0.484	0.793	-0.451
40	-32637.012	-6.143	-1.949	4.194	0.032	-0.307	0.909	-0.514
20	-32637.012	-6.138	-2.098	4.040	0.093	-0.250	0.885	-0.298
0	-32637.016	-6.136	-2.150	3.986	0.131	0.202	0.591	-0.032
-20	-32637.010	-6.139	-2.084	4.055	0.116	-0.271	0.887	-0.390
-40	-32636.979	-6.147	-1.925	4.222	0.066	-0.385	0.908	-0.485
-60	-32636.907	-6.160	-1.724	4.436	0.046	-0.544	0.784	-0.402
-80	-32636.849	-6.170	-1.545	4.625	0.089	-0.778	0.609	-0.171
-100	-32636.851	-6.170	-1.555	4.615	0.073	-0.759	0.679	0.053
-120	-32636.907	-6.159	-1.745	4.415	0.033	-0.553	0.843	0.045
-140	-32636.951	-6.150	-1.947	4.203	0.045	-0.450	0.960	-0.084
-160	-32636.910	-6.143	-2.099	4.044	0.118	-0.452	1.005	-0.132
-180	-32636.840	-6.138	-2.153	3.985	0.155	0.105	0.612	-0.454

Table 9. Structural parameters and charges (C8, N2, C9, C10) for T(C8–N2–C9–C10) angles.

Torsion2	E _{tot} (eV)	HOMO	LUMO	Gap _{H-L} (eV)	C8	N2	C9	C10
180	-32637.020	-6.138	-2.087	4.051	0.086	-0.126	-0.765	0.267
160	-32636.983	-6.139	-2.097	4.042	0.116	-0.093	-0.666	0.188
140	-32636.958	-6.147	-2.117	4.030	0.204	-0.071	-0.565	0.062
120	-32636.957	-6.157	-2.133	4.025	0.246	-0.079	-0.424	-0.049
100	-32636.932	-6.141	-2.131	4.010	0.205	-0.039	-0.522	0.086
80	-32636.670	-6.094	-2.114	3.980	0.155	-0.041	-0.723	0.253
60	-32635.191	-5.841	-2.074	3.767	0.176	-0.118	-0.664	0.199
40	-32630.975	-4.713	-1.954	2.759	0.115	-0.170	-0.585	0.087
20	-32630.783	-3.131	-1.586	1.545	-0.279	-0.210	-0.568	0.036
0	-32628.338	-3.153	-1.981	1.172	-0.356	-0.212	-0.540	-0.020
-20	-32631.368	-2.915	-1.510	1.405	-0.419	-0.197	-0.486	-0.381
-40	-32635.063	-3.299	-1.712	1.587	-0.334	-0.121	-0.643	0.012
-60	-32636.214	-4.818	-2.025	2.793	-0.158	-0.099	-0.741	0.197
-80	-32636.405	-5.764	-2.096	3.668	-0.116	-0.062	-0.715	0.243
-100	-32636.435	-5.999	-2.137	3.863	-0.095	-0.029	-0.535	0.131
-120	-32636.460	-6.074	-2.158	3.916	-0.028	-0.045	-0.397	-0.010
-140	-32636.501	-6.096	-2.157	3.939	0.017	-0.052	-0.463	-0.020
-160	-32636.539	-6.091	-2.140	3.951	-0.066	-0.034	-0.600	0.100
-180	-32637.020	-6.082	-2.123	3.959	-0.131	-0.059	-0.713	0.218

It must be noted that the T(C8–N2–C9–C10) torsion angles in this compound is near to its value in the global minimum.

3.5. Mulliken charge analysis

Mulliken populations yield one of the simplest pictures of charge distribution and Mulliken charges render net atomic populations in the molecules. In order to investigate the electron population of each atom of the title compound, Mulliken charges of the compound were calculated using the DFT/B3LYP method with the 6-311++G (d,p) basis set.

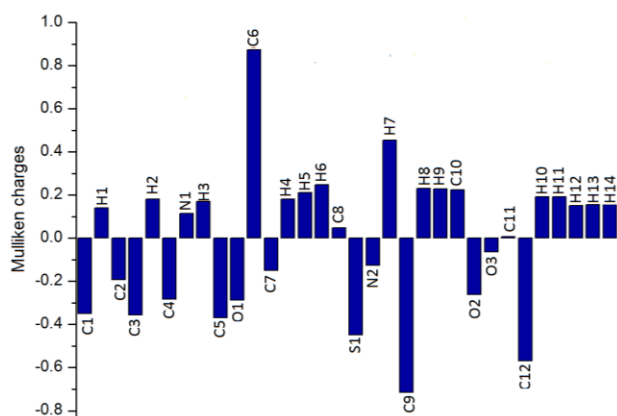


Fig. 5. Mulliken charges of the title compound.

Mulliken charge plot has shown in Fig. 5. The Mulliken analysis shown that the benzene carbon atoms are negative, whereas C6, C8, C10 (adjacent to the oxygen atoms) and C11 atoms are positively charged. All the hydrogen atoms and N1 atom have positive charges. while N2, S1, O2 and O3 atoms have negative charges. The maximum positive atomic charge is obtained for C6 atom of carbonyl group when compared with all other atoms. This is due to the attachment of negatively charged C1, C5 and C7 atoms.

3.6. Molecular Electrostatic Potential Analysis

Electrostatic potential maps give us to visualize the charge distributions of molecules and charge related properties of molecules. They also allow us to visualize the size, shape and bond character of molecules. This knowledge of the charge distributions can be used to determine how molecules interact with one another.

In the majority of the molecular electrostatic potential (MEP), while areas of low potential, red, are characterized by an abundance of electrons, areas of high potential, blue, are characterized by a relative absence of electrons. Intermediary colors represent intermediary electrostatic potentials. This indicates that the electronegativity difference is not very great. Also the MEP is very useful in research of molecular structure with its physiochemical property relationship [52]. In this study, 3D plots of MEP of the title molecule illustrated in Fig. 6.

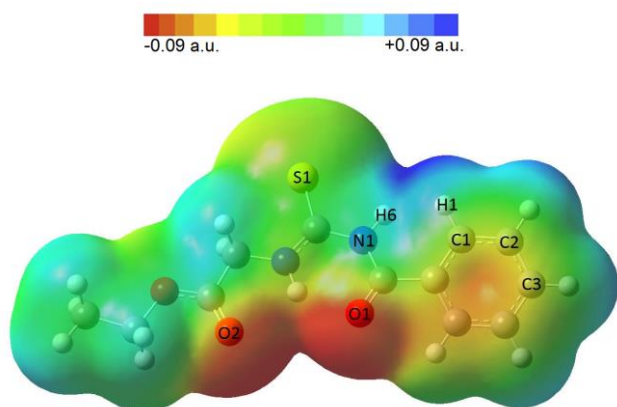


Fig. 6 The total electron density mapped with the electrostatic potential surface of the title compound.

As can be seen from the Fig. 6, oxygen atoms would have a higher electron density than others. The negative regions in the molecule were found around the keto group (O2 atom) and benzene ring. The negative $V(r)$ values is almost -0.089 a.u. between O1 and O2 atom which is the most negative region. Therefore, we can predicted that an electrophile would preferably attack of the title molecule at the O atoms.

On the other hand, the greatest positive region is localized on the between H1 and H6 atoms in which value is $+0.062$ a.u., H atoms bonded benzene the second most (change from $+0.043$ a.u. to $+0.061$ a.u.), and methyle group has the smallest positive regione ($+0.033$ a.u.). In the electrostatic potential map, while the semi-spherical blue shapes that emerge from the edges of the electrostatic potential map are hydrogen atoms, red region is inside of the benzene ring (-0.047 a.u.). The MEP results of the title compound are in agreement with the literature [52].

4. Conclusions

Attempts have been made in the present work for the structure parameters and frequency assignments for the compound ethyl 2-(3-benzoylthioureido)-acetate. Comparison of the structural parameters with experimental results show that DFT/B3LYP basis set is more suitable for these molecular systems. The optimized geometry parameters calculated at B3LYP/6-311++G(d,p) are slightly larger than those calculated at HF/6-311++G(d,p) level and the HF calculated values coincides well compared with the experimental data. The HOMO and LUMO analysis is studied to determine the charge transfer within the molecule. The lowering of the HOMO–LUMO energy gap value has substantial influence on the intramolecular charge transfer and bioactivity of the molecule. Therefore vibrational frequencies, molecular electrostatic potential and atomic charge analysis of the title compound were performed by DFT(B3LYP) levels of theory utilizing 6-311++G(d,p) basis sets. From the MEP it is evident that, the negative potential sites is on keto group and the positive potential sites are around the nitrogen and hydrogen atoms.

References

- [1] A. Esteves-Souza, K. Pissinate, M.G. Nascimento, N.F. Grynberga, A. Echevarria, *Bioorg. Med. Chem.* **14**, 492 (2006).
- [2] R. Ziessel, L. Bonardi, P. Retailleau, G. Ulrich, *Org. Chem.* **71**, 3093 (2006).
- [3] D.E. Fuerst, E.N. Jacobsen, *J. Am. Chem. Soc.* **127**, 8964 (2005).
- [4] A.G. Wenzel, E.N. Jacobsen, *J. Am. Chem. Soc.* **124**, 12964 (2002).
- [5] Y. Tang, L. Deng, Y. Zhang, G. Dong, J. Jiahua, J. Chen, Z. Yang, *Org. Lett.* **7**, 1657 (2005).
- [6] C. Fonta, M. Hidalgo, V. Salvado, E. Antico, *Anal. Chim. Acta*, **547**, 255 (2005).
- [7] A. Tadjarodi, F. Adhami, Y. Hanifehpour, M. Yazdi, Z. Moghaddamfard, G. Kickelbick, *Polyhedron* **26**, 4609 (2007).
- [8] S.N. Manjula, N.M. Noolvi, K.V. Parihar, S.A.M. Reddy, V. Ramani, A.K. Gadad, G. Sing, N.G. Kuttu, C.M. Rao, *Eur. J. Med. Chem.* **44**, 2923 (2009).
- [9] Y.F. Yuan, J.T. Wang, M.C. Gimeno, A. Laguna, P.G. Jones, *Inorg. Chim. Acta*, **324**, 309 (2001).
- [10] Y.M. Zhang, T.B. Wei, L. Xian, L.M. Gao, *Phosphorus, Sulphur Silicon Relat. Elem.* **179**, 2007 (2004).
- [11] Y.M. Zhang, T.B. Wei, X.C. Wang, S.Y. Yang, *Indian J. Chem., Sect. B* **37**, 604 (1998).
- [12] W.Q. Zhou, B.L. Li, L.M. Zhu, J.G. Ding, Z. Yong, L. Lu, X.J. Yang, *J. Mol. Struct.* **690**, 145 (2004).
- [13] M. Eweis, S.S. Elkholy, M.Z. Elsabee, *Int. J. Biol. Macromol.* **38**, 1 (2006).
- [14] S. Saeed, M.H. Bhatti, M.K. Tahir, P.G. Jones, *Acta Crystallogr., Sect. E* **64**, 1369 (2008).
- [15] H. Arslan, N. Külçü, U. Flörke, *Spectrochim. Acta Part A.* **64**, 1065 (2006).
- [16] S. Saeed, N. Rashid, P. G. Jones, M. Ali, R. Hussain, *Eur. J. Med. Chem.* **45**, 1323 (2010).
- [17] V. Ravichanran, V. K. Mourya, R. K. Agrawal, *Digest J. Nanomater. and Biostruc.*, **4**, 213 (2009).
- [18] M.S.M. Yusof, M.A. Ibarahim, N. M. Amin, V. Supramaniam, B.M. Yamin, *UKM-ITB VIII*, 263 (2009).
- [19] N. I. M. Halim, K. Kassima, A. H. Fadzila, B. M. Yamin, *APCBEE Procedia* **3**, 129 (2012).
- [20] A. Saeed, M. S. Khan, H. Rafique, M. Shahid, J. Iqbal, *Bioorganic Chemistry* **52**, 1 (2014).
- [21] I. N. Hassan, B. M. Yamin, M. B. Kassim, *Acta Cryst. E* **64**, 1727 (2008).
- [22] R. Bauernschmitt, R. Alhrichs, *J. Chem Phys.* **104**, 9047 (1996).
- [23] A. D. Becke, *J. Chem. Phys.* **98**, 5648 (1993).
- [24] C. Lee, W. Yang, R.G. Parr, *Phys. Rev. B* **37**, 785 (1988).
- [25] M.J. Frisch et al., *Gaussian 09, Revision C.01*, Gaussian, Inc., Wallingford, CT, 2009.
- [26] Chemcraft (version 1.6, build 304), 2009. <<http://www.chemcraftprog.com>>.
- [27] R. Dennington, T. Keith, J.

- Millam, GaussView, Version 5, Semichem Inc., Shawnee Mission, KS, 2009.
- [28] F. H. Allen, O. Kennard, D. G. Watson, L. Brammer, A. G. Orpen, & R. Taylor, *J. Chem. Soc. Perkin Trans.* **2**, 1 (1987).
- [29] P.D. Babu, S. Periandy, S. Mohan, S. Ramalingam, B.G. Jayaprakash, *Spectrochim. Acta Part A* **78**, 168 (2011).
- [30] N. Sundaraganesan, S. Ilakiamani, H. Saleem, P.M. Wojciechowski, D. Michalska, *Spectrochim. Acta Part A* **61**, 2995 (2005).
- [31] V. Krishnakumar, R. John Xavier, *Indian J. Pure. Appl. Phys.* **41**, 597 (2003).
- [32] V. Krishnakumar, N. Prabavathi, *Spectrochim. Acta Part A* **71**, 449 (2008).
- [33] A. Altun, K. Golcuk, M. Kumru, *J. Mol. Struct.:Theochem* **637** 155 (2003).
- [34] S.J. Singh, S.M. Pandey, *Indian J. Pure. Appl. Phys.* **12**, 300 (1974).
- [35] R.N. Singh, S.C. Prasad, *Spectrochim. Acta Part A* **34**, 39 (1974).
- [36] R.M. Silverstein, G. Clayton Bassler, T.C. Morrill, *Spectroscopic Identification of Organic Compounds*, John Wiley, New York, 1991.
- [37] A. Altun, K. Gölçük, M. Kumru, *J. Mol. Struct.:Theochem* **625**, 17 (2003).
- [38] J.R. Durig, M.M. Bergana, H.V. Phan, *J. Ram. Spect.* **22**, 141 (1991).
- [39] G. Litvinov, *Proceedings of the XIII International Conference on Raman Spectroscopy*, Wurzburg, Germany, 1992.
- [40] M. Govindarajan K. Ganasanb, S. Periandyc, S. Mohand, *Spectrochim. Acta Part A* **76**, 12 (2010).
- [41] H. Arslan, Ö. Algül, *Spectrochim. Acta Part A* **70**, 109 (2008).
- [42] V. Arjunan, R. Santhanam, S. Sakiladevi, M.K. Marchewka, S. Mohan, *J. Mol. Struct.:Theochem* **1037**, 305 (2013).
- [43] M.M.J. Tecklenburg, D.J. Kosnak, A. Bhatnagar, D.K. Mohanty, *J. Raman Spectry* **28**, 755 (1997).
- [44] J. Pajazk, M. Rospenk, R. Ramaekers, G. Maes, T. Głowiak, L. Sobczyk, *Chem. Phys.* **278**, 89 (2002).
- [45] M. Arivazhagan, V. Krishnakumar, R. JohnXavier, V. Ilango, K. Balachandran, *Spectrochim. Acta Part A*, **72**, 941 (2009).
- [46] G. Varsanyi, *Vibrational Spectra of Benzene Derivatives*, *Academic Press*, New York, 1969
- [47] R.M. Silverstein, F. X. Webster, *Spectrometric Identification of Organic Compounds*, sixth ed., John Wiley & Sons, New York, 1998.
- [48] Y. Zhang, H. Zhou, Z. Jiang, R. Li, *Spectrochim. Acta Part A*, **83**, 112 (2011).
- [49] N.B. Colthup, L.H. Daly, S.E. Wiberly, *Introduction to Infrared and Raman Spectroscopy*, second ed., Academic Press, New York, 1975.
- [50] E. S. Al-Abdullah, Y. S. Mary, C. Y. Panicker, N. R. El-Brollosy, A. A. El-Emam, C. Van Alsenoy, & A. A. Al-Saadi, *Spectrochim. Acta Part A*, **133**, 639 (2014).
- [51] I. Fleming, *Frontier Orbitals and Organic Chemical Reactions*, Wiley, London, (1976).
- [52] H. Tanak, M. Toy, *J. Mol. Struct.:Theochem* **1068**, 189 (2014).

*Corresponding author: meryem.evecen@amasya.edu.tr